

Original Article

Myosin VI contributes to malignant proliferation of human glioma cells

Rong Xu^{1,#}, Xu-hao Fang^{2,#}, and Ping Zhong^{1,*}

¹Neurosurgical Department of Huashan Hospital, Fudan University, Shanghai 200040, ²Neurosurgical Department of Huadong Hospital, Fudan University, Shanghai 200040, China

ARTICLE INFO

Received October 31, 2014

Revised February 13, 2015

Accepted March 3, 2015

*Correspondence

Ping Zhong

E-mail: dr_zhongping@163.com

Key Words

Cell cycle

Glioma

Myosin VI

Proliferation

ShRNA

ABSTRACT Previously characterized as a backward motor, myosin VI (*MYO6*), which belongs to myosin family, moves toward the minus end of the actin track, a direction opposite to all other known myosin members. Recent researches have illuminated the role of *MYO6* in human cancers, particularly in prostate cancer. However, the role of *MYO6* in glioma has not yet been determined. In this study, to explore the role of *MYO6* in human glioma, lentivirus-delivered short hairpin RNA (shRNA) targeting *MYO6* was designed to stably down-regulate its endogenous expression in glioblastoma cells U251. Knockdown of *MYO6* significantly inhibited viability and proliferation of U251 cells *in vitro*. Moreover, the cell cycle of U251 cells was arrested at G0/G1 phase with the absence of *MYO6*, which could contribute to the suppression of cell proliferation. In conclusion, we firstly identified the crucial involvement of *MYO6* in human glioma. The inhibition of *MYO6* by shRNA might be a potential therapeutic method in human glioma.

[#]These authors contributed equally to this work.

INTRODUCTION

Gliomas are the most common primary tumors affecting the adult central nervous system, characterized by high morbidity and mortality as well as a high recurrence rate [1]. Gliomas are presumed to arise from mature glia or neural stem cells and diffusely infiltrate the surrounding tissues [2], making surgical resection very difficult. Survival from gliomas depends on the tumor type and grades of malignancy [3]. The World Health Organization (WHO) defines four brain tumor classes (I, II, III, IV) on the basis of their morphological features and predicted clinical behaviour. The most lethal is grade IV glioblastoma (GBM), with a five-year survival rate of less than 10% due to difficulties in complete resection and the low sensitivity to radiotherapy and chemotherapy [4-6]. Hence, there are ongoing efforts to increase the understanding of glioma malignant progression.

Myosins are actin-based motor proteins, coupling ATP

hydrolysis to mechanical motion along actin filaments. Many myosin family have been implicated as molecular motors, which play important roles in the transport of intracellular organelles [7]. They are known to contribute to essential cellular functions, including secretion, cell division, differentiation, and migration [8]. Myosin VI (*MYO6*), in contrast to all other myosins, is the only identified member of this protein family that is capable of moving toward the minus end of the actin filament [9]. *MYO6* has three functional domains: an N-terminal motor domain or head domain, a C-terminal tail domain and a so-called neck region. The N-terminal motor domain has ATPase activity and binds to actin molecules, whereas the tail domain contributes to the dimerization of myosin molecules and cargo binding. The neck region contains light chain- or calmodulin-binding IQ motifs [10, 11]. *MYO6* is thought to transport endocytic vesicles into the cell, functions in a variety of intracellular processes such as vesicular membrane traffic, cytokinesis and migration [12]. Moreover, *MYO6* is required in the process of the fusion of



This is an Open Access article distributed under the terms of the Creative Commons Attribution Non-Commercial License, which permits unrestricted non-commercial use, distribution, and reproduction in any medium, provided the original work is properly cited.
Copyright © Korean J Physiol Pharmacol, pISSN 1226-4512, eISSN 2093-3827

Author contributions: P.Z. and R.X. conceived and designed the study. R.X. and X.F. performed the experiments. R.X. and X.F. wrote the paper. P.Z., R.X. and X.F. reviewed and edited the manuscript. All authors read and approved the manuscript.

endosome and lysosome in epithelial cells, which contributes to the maintenance of epithelial barrier function [13].

MYO6 plays an important role in the generation and maintenance of hair cell stereocilia [14]. Mutations in the *MYO6* gene cause both autosomal dominant non-syndromic hearing loss (DFNA22) and autosomal recessive non-syndromic hearing loss (DFNB37) [15,16]. Szczyrba et al. show that *MYO6* is a target for both miR-143 and miR-145. The fact that a downregulation of miR-143 and miR-145 has been reported in several studies including patients with different tumors and different ethnic backgrounds points to the possibility that *MYO6* overexpression may be an important tumorigenic event in several tumors, including breast, ovarian, and prostate cancer [17]. Previous studies demonstrated that *MYO6* expression levels were increased in prostate cancer [18,19]. According to microarray analyses, scientists found that *MYO6* had a high-resolution copy number and gene expression in head and neck squamous cell carcinoma cell lines of tongue and larynx [20]. In general, all of these findings showed that *MYO6* played importance functional roles in carcinogenesis. Yet, the role of *MYO6* in glioma has not yet been determined.

In this study, to explore the role of *MYO6* in human glioma, lentivirus-delivered short hairpin RNA (shRNA) targeting *MYO6* was used to stably down-regulate its endogenous expression in glioblastoma cells U251. Knockdown of *MYO6* significantly inhibited viability and proliferation of U251 cells *in vitro*. Therefore, *MYO6* contributes to malignant proliferation of glioma cells, and the inhibition of *MYO6* by shRNA might be a potential therapeutic method in glioma.

METHODS

Materials

Dulbecco's modified Eagle's medium (DMEM) was obtained from Hyclone (Logan, Utah, USA, cat no.SH30243.01B+). Fetal bovine serum (FBS) was obtained from Biowest (Loire Valley, France, cat no.S1810). Lipofectamine 2000 and TRIzol[®] Reagent was purchased from Invitrogen (Carlsbad, CA, USA). M-MLV Reverse Transcriptase was purchased from Promega (Madison, WI, USA). All other chemicals were obtained from Sigma-Aldrich (St. Louis, MO, USA). The lentiviral vector (pFH-L) and packaging vectors (pVSVG-I and pCMVΔR8.92) were purchased from Hollybio (Shanghai, China). The antibodies used were as following: mouse anti-*MYO6* antibody (1:1,000 dilution; Sigma-Aldrich, cat no.M0691), rabbit anti-GAPDH antibody (1:40,000 dilution; Proteintech Group, Inc., cat no.10494-1-AP), horseradish peroxidase-conjugated goat anti-mouse (1:5,000 dilution; Santa Cruz, cat no.SC-2005) and goat anti-rabbit (1:5,000 dilution; Santa Cruz, cat no.SC-2054) secondary antibodies.

Cell culture

Human glioblastoma cells U251 and human embryonic kidney cells 293T were purchased from the Cell Bank of Chinese Academy of Science (Shanghai, China). In this study, 293T cells were used to produce replication-incompetent lentiviral particles, while U251 cells were used as target for *in vitro* infection experiments. These cell lines were maintained in DMEM containing 10% FBS at 37°C in humidified atmosphere of 5% CO₂.

Lentivirus-delivered short hairpin RNA transduction

The shRNA sequence targeting human *MYO6* gene (NCBI accession number: NM_004999) was 5'-GTGAATCCAGAGA TAAGTTTACTCGAGTAACTTATCTCTGGATTCACTTT TT-3', which was subjected to BLAST analysis against the human genome database to eliminate cross-silence phenomena with nontarget genes. A scrambled fragment (5'-GCGGAGGGTTTG AAAGAATATCTCGAGATATTTCTTTCAAACCCTCCGCTTT TTT-3') that has no significant homology with mouse or human gene sequences was used as a negative control. The shRNAs were cloned into the pFH-L vector by use of NheI/PacI restriction sites, which was then transfected into 293T cells with packaging vectors (pVSVG-I and pCMVΔR8.92) using Lipofectamine 2000 according to the manufacturer's instructions. The supernatant was collected 48 h later, centrifuged (4000 g, 4°C, 10 min) to remove cell debris, filtered through 0.45-μm cellulose acetate filters, and then concentrated again (4000 g, 4°C, 15 min). U251 cells were dispensed into 6-well plates at a density of 50,000 cells per well and transduced with shRNA-expressing lentivirus (shCon or sh*MYO6*) at a multiplicity of infection (MOI) of 10. The lentiviral vectors expressed green fluorescence protein (GFP), which allowed for measurement of infection efficiency in transduced cells.

Quantitative real-time PCR analysis

U251 cells were harvested after lentivirus transduction for four days. Total cellular RNA was extracted using Trizol reagent and reversely transcribed to cDNA by M-MLV reverse transcriptase according to the manufacturer's instructions. qPCR products were detected with SYBR Green on BioRad Connet Real-Time PCR platform. qPCR procedure was denaturation at 95°C for 1 min, 40 cycles of denaturation at 95°C for 5s and extension at 60°C for 20 s. β-actin gene was amplified as internal control. Relative quantitation was analyzed by taking the difference ΔC(T) between the C(T) of β-actin and C(T) of *MYO6* and computing $2^{-\Delta\Delta C(T)}$. The following primers were used: *MYO6*, 5'-AATCACTGGCTCACATGCAG-3' (forward) and 5'-AATGCGAGGTTTGTGTCTCC-3' (reverse); β-actin, 5'-GTGGACATCCGCAAAGAC-3' (forward) and

5'-AAAGGGTGTAACGCAACTA-3' (reverse).

Western blotting analysis

U251 cells were harvested after lentivirus transduction for six days. Total protein was extracted with 2×SDS Sample Buffer (100 mM Tris-HCl (pH 6.8), 10 mM EDTA, 4% SDS, 10% Glycine). Equal amounts of lysate (30 µg) in each lane, as determined by the bicinchoninic acid (BCA) assay, were separated by 8% SDS-PAGE and transferred to PVDF membranes. The membranes were blocked with 5% nonfat dry milk in Tris-buffered saline with Tween 20 (TBST) for 1 h at room temperature, and incubated with TBST containing anti-MYO6 or anti-GAPDH antibody overnight at 4°C, followed by incubation with secondary antibody for 1 h at room temperature. The blots were detected using enhanced chemiluminescence (ECL) kit (Amersham) and visualized by exposure to X-ray film. GAPDH was used as a control to verify equal protein loading.

MTT viability assay

To evaluate the effect of MYO6 on glioma cell viability, 3-(4,5-dimethylthiazol-2-yl)-2,5-diphenyl-tetrazolium bromide (MTT) colorimetric assay was performed in U251 cells after lentivirus transduction for four days. Briefly, U251 cells were dispensed into 96-well plates at a concentration of 2,000 per well. The plates were incubated for one to five days at 37°C. On each day, 20 µL of MTT (5 mg/mL) was added and incubated for 4 h. Afterwards, the entire supernatant was discarded and acidic isopropanol (10% SDS, 5% isopropanol and 0.01 mol/L HCl) was added at a volume of 100 µL per well and incubated at 37°C for 10 min. The absorbance at 595 nm of each well was determined using an ELISA reader. Experiments were performed in triplicate.

Colony formation assay

To evaluate the effect of MYO6 on glioma cell proliferation, colony formation assay was performed in U251 cells after lentivirus transduction for four days. Briefly, U251 cells were dispensed into 6-well plates at a concentration of 500 per well. The culture medium was changed at three days intervals. U251 cells were cultured for seven days until the most single colony contains more than 50 cells. The colonies were stained with crystal violet for 20 min, and then washed with water and air-dried. Cell colonies were captured and counted under a microscope.

Fluorescence-activated cell sorting analysis

To evaluate the effect of MYO6 on glioma cell cycle progression, flow cytometry assay was performed in U251 cells after lentivirus transduction for four days. Briefly, U251 cells were dispensed into 6-cm dishes at a concentration of 200,000 per dish. After culture

at 37°C for 40 h, cells were harvested, fixed in 70% ethanol, and stored overnight at 4°C. The cells were then treated with NaCl/Pi staining solution (50 µg/mL PI and 100 µg/mL RNase A). Following incubation for 1 h in the dark at room temperature, cells were analyzed by flow cytometry (FACSCalibur; Becton Dickinson, San Jose, CA, USA). The fractions of the cells in G0/G1, S and G2/M phases were analyzed with dedicated software (Becton Dickinson). Experiments were performed in triplicate and the results were shown as the average.

Cell apoptosis assay

To determine the effect of MYO6 on the rate of cellular apoptosis, Annexin V-APC/7-AAD Apoptosis Detection Kit (KeyGEN BioTECH, #KGA1026) was performed in U251 cells following lentivirus infection for four days. The infected cells were incubated in 6-cm dishes at a density of 3×10⁴ cells/dish. Then, the cells were harvested, washed with PBS for three times and suspended in 100 ml of annexin binding buffer, 5 ml of annexin V-APC solution, and 2 ml of the PI solutions after five days of culture. The cells were seeded in the medium for 15 min in the dark at room temperature. Flow cytometry assay was performed on FACS caliber II sorter and Cell Quest FACS system (BD Biosciences, USA) to analyze the fluorescence-stained cells and non-infected cells were used to set the background.

Statistical analysis

Statistical analysis was performed using SPSS 16.0 software package (SPSS Inc, Chicago, IL, USA). All data were expressed as mean±standard deviation (SD). Differences between two groups were analyzed by Student's t-test and a p value of less than 0.05 was considered statistically significant.

RESULTS

Knockdown of MYO6 expression with lentivirus-delivered shRNA

U251 cells were transduced with shRNA-expressing lentivirus (shCon or shMYO6). GFP expression was observed by fluorescent microscopy four days post-transduction. As depicted in Fig. 1A, over 80% of cells expressed GFP in both shCon and shMYO6 groups, indicating a successful infection rate. The inhibitory effect of MYO6 shRNA on its endogenous expression in U251 cells was examined by qRT-PCR and western blotting. As demonstrated in Fig. 1B, the mRNA level of MYO6 was significantly reduced in U251 cells infected with shMYO6 with a knockdown efficiency of 65.7%, in contrast to cells infected with shCon. Immunoblot also verified the down-regulation of MYO6 expression at protein level (Fig. 1C). Therefore, lentivirus-delivered shRNA could specifically

deplete endogenous *MYO6* expression in glioblastoma cells.

Effects of *MYO6* knockdown on cell viability and proliferation

We next examined the effects of *MYO6* knockdown on viability and proliferation of U251 cells. After infection of *MYO6* shRNA, MTT assay was performed in U251 cells for five consecutive days. As shown in Fig. 2A, the number of viable cells infected with sh*MYO6* was much fewer than that in infected shCon ($p < 0.001$), indicating that knockdown of *MYO6* could strongly decrease the viability of glioblastoma cells.

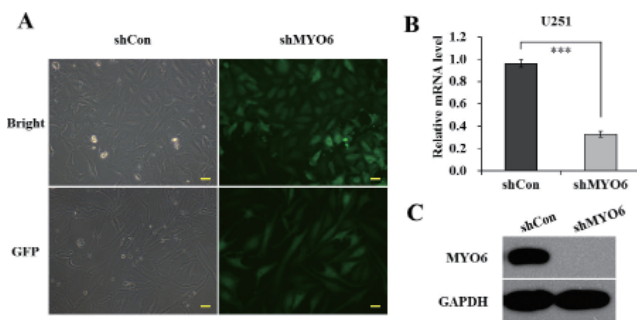


Fig. 1. Lentivirus-delivered shRNA targeting *MYO6* depleted its endogenous expression in U251 cells. (A) Evaluation of the lentivirus transduction rate, which was more than 80% as calculated by cellular enumeration using fluorescence and light microscopy. (B) Quantitative analysis of *MYO6* knockdown efficiency in U251 cells assessed by qRT-PCR. β -actin gene was used as an internal control. (C) Representative immunoblot showing *MYO6* knockdown efficiency determined in U251 cells. GAPDH protein was used as an internal control. Data are mean \pm SD ($n=3$; t-test). * $p < 0.001$; scale bar, 100 μ m.

Moreover, colony formation assay was performed and representative photographs were presented as Fig. 2B. Crystal violet staining and fluorescence expression showed that both the size of monoclonal and the number of total colonies were decreased in sh*MYO6*-infected cells. The colony formation ability was significantly impaired, with a reduction by 32.3% in U251 cells after *MYO6* knockdown ($p < 0.001$, Fig. 2C), indicating that knockdown of *MYO6* could strongly disrupt the colony formation of glioblastoma cells.

Effects of *MYO6* knockdown on cell cycle control

To test the mechanism by which *MYO6* modulating cell proliferation, the flow cytometry assay was used to determine the cell cycle of U251 cells. Representative images of cell cycle distribution were presented as Fig. 3A. As depicted in Fig. 3B, the cell percentage of G0/G1 phase was increased from 49.66% in shCon-infected cells to 67.10% in sh*MYO6*-infected cells. In contrast, the cell percentage of S phase was decreased from 25.20% in shCon-infected cells to 8.19% in sh*MYO6*-infected cells. This indicated that Lv-sh*MYO6* could strongly block ($p < 0.001$) the cell cycle progression of glioblastoma cells. Taken together, these results suggested knockdown of *MYO6* could inhibit glioblastoma cell proliferation by inducing G0/G1 phase cell cycle arrest.

Effects of *MYO6* knockdown on cell apoptosis

To further investigate the effect of *MYO6* on cell apoptosis, we then applied Annexin V/PI double staining in U251 cells after lentivirus infection (Fig. 4A). Annexin V vs PI plots from

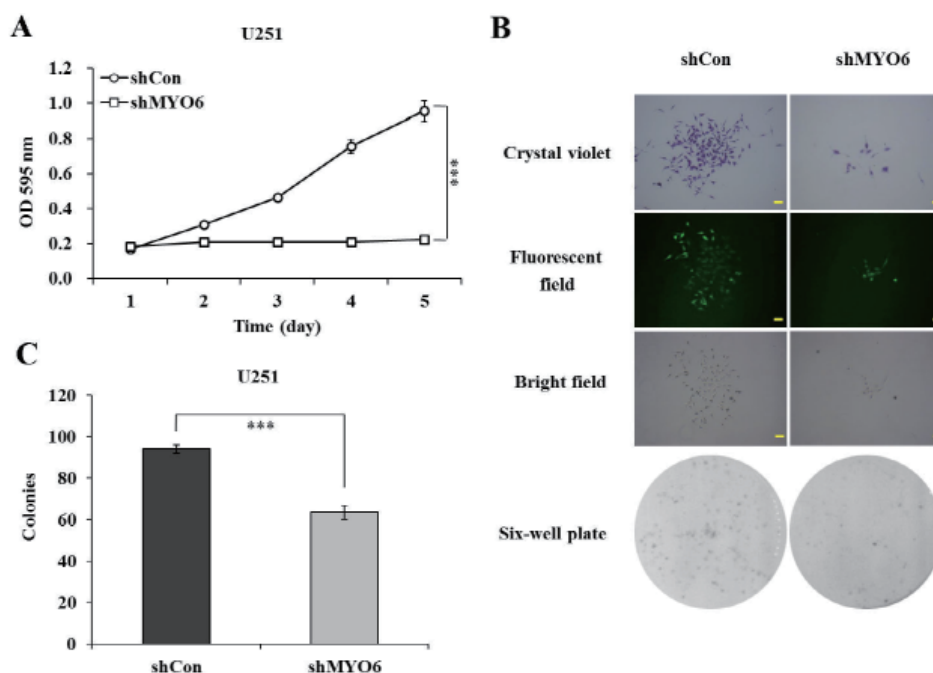


Fig. 2. Knockdown of *MYO6* inhibits viability and proliferation of glioblastoma U251 cells. (A) MTT showing growth curves determined in U251 cells. The number of viable cells was much fewer in the sh*MYO6* group than in the shCon group. (B) Representative colony formation showing clonogenic survival determined in U251 cells. (C) The number of colonies was much fewer in the sh*MYO6* group than in the shCon group. Data are mean \pm SD ($n=3$; t-test). * $p < 0.001$; scale bar, 250 μ m.

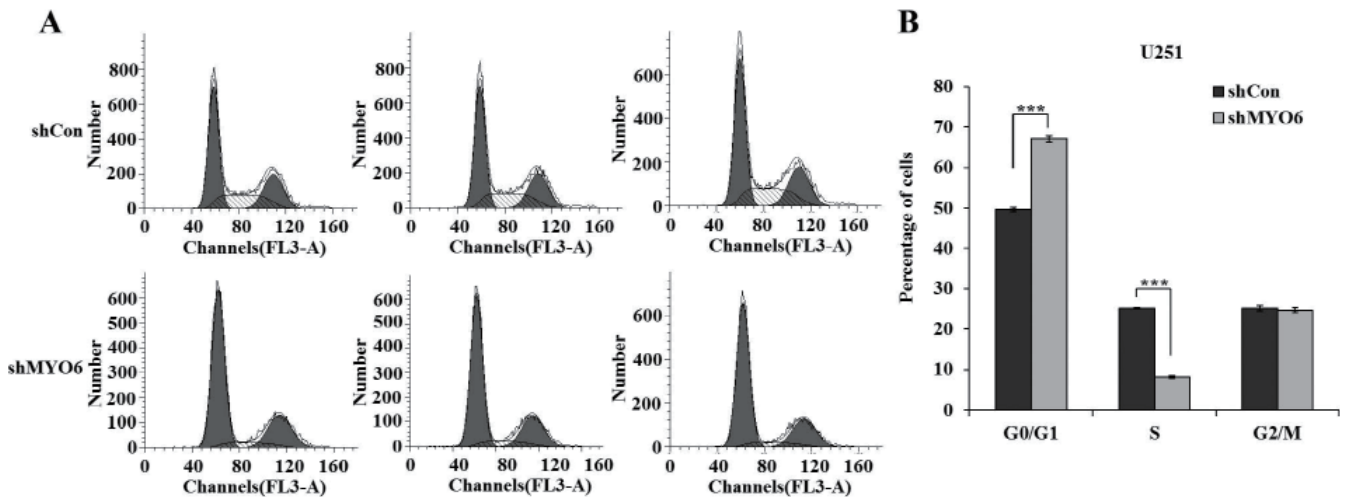


Fig. 3. Knockdown of MYO6 arrests cell cycle progression in U251 cells. (A) Comparison of the cell population in G0/G1, S and G2/M phase between shCon and shMYO6 groups assessed by flow cytometry. (B) The percentage of cells in G0/G1 phase was significantly higher in the shMYO6 group than in the shCon group, while the percentages of cells in S phase was simultaneously reduced. Data are mean±SD (n=3; t-test). ***p<0.001.

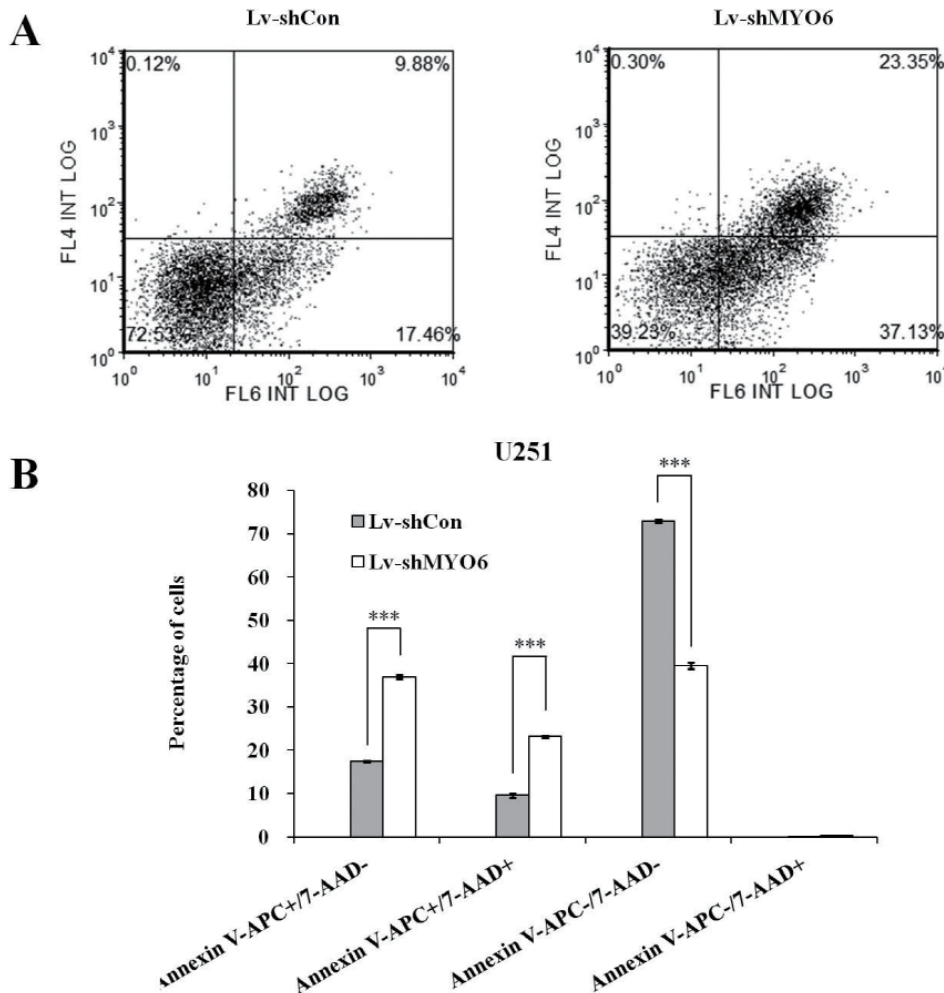


Fig. 4. Effect of MYO6 knockdown on cell apoptosis. (A) Cytochrome of Annexin V-APC binding vs. 7-AAD uptake in U251 cells following lentivirus infection in shCon and shMYO6 groups. (B) Quantification of apoptotic cells in U251 cells by FACS. Annexin V+/7-AAD-: early apoptotic cells; Annexin V+/7-AAD+: late apoptotic cells; Annexin V-/7-AAD-: viable cells; Annexin V-/7-AAD+: cells in necrosis.

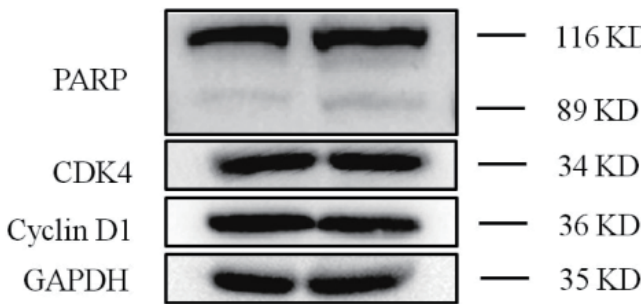


Fig. 5. Knockdown of *MYO6* regulate the expression of cell cycle markers. The expression alterations of cell cycle markers in glioma cells was confirmed by using western blotting, including CDK4, Cyclin D1 and PARP.

the gated cells showed the populations corresponding to early (Annexin V+/PI-), and late (Annexin V+/PI+), viable (Annexin V-/PI-) and necrotic (Annexin V-/PI+) apoptotic cells. As shown in Fig. 4B, apoptotic cells (early apoptosis and late apoptosis) were dramatically augmented in the sh*MYO6* group, as compared to shCon and Con groups. Therefore, the results reveal that *MYO6* inhibition induced a strong pro-apoptotic effect in glioblastoma cells. We may infer that *MYO6* knockdown suppressed glioblastoma cell growth through inducing cell cycle arrest and apoptosis.

Effect of *MYO6* knockdown on the cell cycle regulators

To investigate the underlying mechanism for cell cycle arrest and apoptosis, we have further detected the alterations of the cell cycle regulators including CDK4, Cyclin D1 and PARP. CDK4 and Cyclin D1 were typical cell cycle arrest-related proteins in G0/G1 phase and the expression level of PARP was closely associated with cell apoptosis. As shown in Fig. 5, knockdown of *MYO6* led to the cleavage of PARP. However, knockdown of *MYO6* didn't decrease the expression of CDK4 and Cyclin D1, which was G0/G1 phase cell cycle arrest-related proteins. Therefore, we suggested that knockdown of *MYO6* could induce cell apoptosis via cleavage of PARP.

DISCUSSION

Previous studies showed upregulation of *MYO6* after an extremely traumatic stress experience, along with a delayed decrease in 5-bromo-2'-deoxyuridine incorporation in the murine hippocampus, a brain structure believed to undergo adult neurogenesis [21]. A recent report demonstrates that *MYO6* selectively inhibits cellular proliferation required for self-replication in undifferentiated P19 cells and suggests that further evaluation of *MYO6* expression will be beneficial for the development of drugs useful for the prophylaxis and therapy of

diverse neurodegenerative and neuropsychiatric diseases [22]. This novel connection should stimulate a thorough investigation of the unique functional properties of *MYO6* in brain tumors. In this study, for the first time, we identified the functional role of *MYO6* in human glioma. Lentivirus-delivered short hairpin RNA (shRNA) targeting *MYO6* strongly inhibited viability and proliferation of glioblastoma cells U251.

The acto-myosin contraction is precisely regulated to ensure that cytokinesis takes place properly during cell division, which is one of the most tightly controlled steps of the cell cycle [23]. It should be noticed that other myosin superfamily members also play roles in cell cycle control. Non-muscle myosin II (NMII) has pivotal roles in different cellular activities, such as cell division, migration and differentiation. Inhibition of NMII leads to G0/G1 arrest in Wharton's jelly-derived mesenchymal stromal cells [24]. In addition, *MYO16* depletion results in altered cell cycle distribution in Rat2 cells [25]. In this study, knockdown of *MYO6* also affected cell cycle progression in U251 cells and led to an increase in the percentage of cells in G0/G1 phase with a corresponding reduction in the percentage of cells in S phase, which could contribute to the suppression of cell proliferation., although CDK4 and Cyclin D1 have no obvious change. Depletion of *MYO6* induced a remarkable pro-apoptotic effect in U251 cells. Furthermore, western blotting showed that knockdown of *MYO6* in glioma cells induced cell apoptosis via cleavage of PARP.

It has been suggested that overexpression of *MYO6* may promote tumor growth and invasion including prostate, ovarian and squamous cell carcinoma[20,26-28]. The specific inhibition of *MYO6* by small interfering RNA transfection of LNCaP prostate cancer cells leads to decreased anchorage-dependent cell growth and cell migration *in vitro* [27]. Depletion of *MYO6* expression was also accompanied by global gene expression changes reflective of attenuated tumorigenic potential, as marked by a nearly 10-fold induction of TXNIP (VDUP1), a tumor suppressor with decreased expression in prostate cancer specimens. A recent research reported that knockdown of *MYO6* markedly reduced the secretion of prostate-specific antigen (PSA) and vascular endothelial growth factor (VEGF) [29]. Further investigation should focus on the molecular mechanism underlying the effect of *MYO6* on glioma growth and metastasis.

In conclusion, we firstly identified the crucial involvement of *MYO6* in human glioma. *MYO6* could facilitate glioma malignant proliferation *in vitro* and the inhibition of *MYO6* by shRNA might be a potential therapeutic method in human glioma.

CONFLICT OF INTERESTS

The authors declare no conflict of interests.

REFERENCES

- Annibaldi D, Whitfield JR, Favuzzi E, Jauset T, Serrano E, Cuartas I, Redondo-Campos S, Folch G, González-Juncà A, Sodir NM, Massó-Vallés D, Beaulieu ME, Swigart LB, Mc Gee MM, Somma MP, Nasi S, Seoane J, Evan GI, Soucek L. Myc inhibition is effective against glioma and reveals a role for Myc in proficient mitosis. *Nat Commun.* 2014;5:4632.
- Huse JT, Holland EC. Targeting brain cancer: advances in the molecular pathology of malignant glioma and medulloblastoma. *Nat Rev Cancer.* 2010;10:319-331.
- Constantin A, Elkhalel A, Jalbert L, Srinivasan R, Cha S, Chang SM, Bajcsy R, Nelson SJ. Identifying malignant transformations in recurrent low grade gliomas using high resolution magic angle spinning spectroscopy. *Artif Intell Med.* 2012;55:61-70.
- Stupp R, Hegi ME, Mason WP, van den Bent MJ, Taphoorn MJ, Janzer RC, Ludwin SK, Allgeier A, Fisher B, Belanger K, Hau P, Brandes AA, Gijtenbeek J, Marosi C, Vecht CJ, Mokhtari K, Wesseling P, Villa S, Eisenhauer E, Gorlia T, Weller M, Lacombe D, Cairncross JG, Mirimanoff RO; European organisation for research and treatment of cancer brain tumour and radiation oncology groups; national cancer institute of Canada clinical trials group. Effects of radiotherapy with concomitant and adjuvant temozolomide versus radiotherapy alone on survival in glioblastoma in a randomised phase III study: 5-year analysis of the EORTC-NCIC trial. *Lancet Oncol.* 2009;10:459-466.
- Mirimanoff RO. High-grade gliomas: reality and hopes. *Chin J Cancer.* 2014;33:1-3.
- Qiu ZK, Shen D, Chen YS, Yang QY, Guo CC, Feng BH, Chen ZP. Enhanced MGMT expression contributes to temozolomide resistance in glioma stem-like cells. *Chin J Cancer.* 2014;33:115-122.
- Seog DH, Han J. Sorting nexin 17 interacts directly with kinesin superfamily KIF1Bbeta protein. *Korean J Physiol Pharmacol.* 2008;12:199-204.
- Hartman MA, Finan D, Sivaramakrishnan S, Spudich JA. Principles of unconventional myosin function and targeting. *Annu Rev Cell Dev Biol.* 2011;27:133-155.
- Wells AL, Lin AW, Chen LQ, Safer D, Cain SM, Hasson T, Carragher BO, Milligan RA, Sweeney HL. Myosin VI is an actin-based motor that moves backwards. *Nature.* 1999;401:505-508.
- Buss F, Spudich G, Kendrick-Jones J. Myosin VI: cellular functions and motor properties. *Annu Rev Cell Dev Biol.* 2004;20:649-676.
- Friedman TB, Griffith AJ. Human nonsyndromic sensorineural deafness. *Annu Rev Genomics Hum Genet.* 2003;4:341-402.
- Buss F, Kendrick-Jones J. How are the cellular functions of myosin VI regulated within the cell? *Biochem Biophys Res Commun.* 2008;369:165-175.
- Liao YW, Wu XM, Jia J, Wu XL, Hong T, Meng LX, Wu XY. Myosin VI contributes to maintaining epithelial barrier function. *J Biomed Sci.* 2013;20:68.
- Self T, Sobe T, Copeland NG, Jenkins NA, Avraham KB, Steel KP. Role of myosin VI in the differentiation of cochlear hair cells. *Dev Biol.* 1999;214:331-341.
- Ahmed ZM, Morell RJ, Riazuddin S, Gropman A, Shaikat S, Ahmad MM, Mohiddin SA, Fananapazir L, Caruso RC, Husnain T, Khan SN, Riazuddin S, Griffith AJ, Friedman TB, Wilcox ER. Mutations of MYO6 are associated with recessive deafness, DFNB37. *Am J Hum Genet.* 2003;72:1315-1322.
- Melchionda S, Ahituv N, Bisceglia L, Sobe T, Glaser F, Rabionet R, Arbones ML, Notarangelo A, Di Iorio E, Carella M, Zelante L, Estivill X, Avraham KB, Gasparini P. MYO6, the human homologue of the gene responsible for deafness in Snell's waltzer mice, is mutated in autosomal dominant nonsyndromic hearing loss. *Am J Hum Genet.* 2001;69:635-640.
- Szczyrba J, Löprich E, Wach S, Jung V, Unteregger G, Barth S, Grobholz R, Wieland W, Stöhr R, Hartmann A, Wullich B, Grässer F. The microRNA profile of prostate carcinoma obtained by deep sequencing. *Mol Cancer Res.* 2010;8:529-538.
- Wei S, Dunn TA, Isaacs WB, De Marzo AM, Luo J. GOLPH2 and MYO6: putative prostate cancer markers localized to the Golgi apparatus. *Prostate.* 2008;68:1387-1395.
- Demichelis F, Setlur SR, Beroukhir R, Perner S, Korbel JO, Lafargue CJ, Pflueger D, Pina C, Hofer MD, Sboner A, Svensson MA, Rickman DS, Urban A, Snyder M, Meyerson M, Lee C, Gerstein MB, Kuefer R, Rubin MA. Distinct genomic aberrations associated with ERG rearranged prostate cancer. *Genes Chromosomes Cancer.* 2009;48:366-380.
- Järvinen AK, Autio R, Kilpinen S, Saarela M, Leivo I, Grénman R, Mäkitie AA, Monni O. High-resolution copy number and gene expression microarray analyses of head and neck squamous cell carcinoma cell lines of tongue and larynx. *Genes Chromosomes Cancer.* 2008;47:500-509.
- Tamaki K, Kamakura M, Nakamichi N, Taniura H, Yoneda Y. Upregulation of Myo6 expression after traumatic stress in mouse hippocampus. *Neurosci Lett.* 2008;433:183-187.
- Takarada T, Kou M, Nakamichi N, Ogura M, Ito Y, Fukumori R, Kokubo H, Acosta GB, Hinoi E, Yoneda Y. Myosin VI reduces proliferation, but not differentiation, in pluripotent P19 cells. *PLoS One.* 2013;8:e63947.
- Lafaurie-Janvore J. Temporal regulation of abscission, the last step of cell division. *Biol Aujourd'hui.* 2013;207:133-148.
- Sharma T, Kumari P, Pincha N, Mutukula N, Saha S, Jana SS, Ta M. Inhibition of non-muscle myosin II leads to G0/G1 arrest of Wharton's jelly-derived mesenchymal stromal cells. *Cytotherapy.* 2014;16:640-652.
- Cameron RS, Liu C, Pihkala JP. Myosin 16 levels fluctuate during the cell cycle and are downregulated in response to DNA replication stress. *Cytoskeleton (Hoboken).* 2013;70:328-348.
- Knudsen B. Migrating with myosin VI. *Am J Pathol.* 2006;169:1523-1526.
- Dunn TA, Chen S, Faith DA, Hicks JL, Platz EA, Chen Y, Ewing CM, Sauvageot J, Isaacs WB, De Marzo AM, Luo J. A novel role of myosin VI in human prostate cancer. *Am J Pathol.* 2006;169:1843-1854.
- Yoshida H, Cheng W, Hung J, Montell D, Geisbrecht E, Rosen D, Liu J, Naora H. Lessons from border cell migration in the Drosophila ovary: A role for myosin VI in dissemination of human ovarian cancer. *Proc Natl Acad Sci U S A.* 2004;101:8144-8149.
- Puri C, Chibalina MV, Arden SD, Kruppa AJ, Kendrick-Jones J, Buss F. Overexpression of myosin VI in prostate cancer cells enhances PSA and VEGF secretion, but has no effect on endocytosis. *Oncogene.* 2010;29:188-200.